

## Advantages of using high-temperature cuprate superconductor heterostructures in the search for Majorana fermions

P. Lucignano,<sup>1,2</sup> A. Mezzacapo,<sup>3</sup> F. Tafuri,<sup>4,5</sup> and A. Tagliacozzo<sup>2,5</sup>

<sup>1</sup>CNR-ISC, via Fosso del Cavaliere 100, I-00133 Roma, Italy

<sup>2</sup>Dipartimento di Scienze Fisiche, Università di Napoli "Federico II", Monte S. Angelo, I-80126 Napoli, Italy

<sup>3</sup>Departamento de Química Física, Universidad del País Vasco UPV/EHU, Apartado 644, E-48080 Bilbao, Spain

<sup>4</sup>Dipartimento Ingegneria dell'Informazione, Seconda Università di Napoli, I-81031 Aversa (CE), Italy

<sup>5</sup>CNR-SPIN, Monte S. Angelo–vai Cinthia, I-80126 Napoli, Italy

(Received 30 April 2012; revised manuscript received 2 October 2012; published 11 October 2012)

We propose an alternative platform to observe Majorana bound states in solid-state systems. High-critical-temperature cuprate superconductors can induce superconductivity, by the proximity effect, in quasi-one-dimensional nanowires with strong spin-orbit coupling. They favor a wider and more robust range of conditions to stabilize Majorana fermions due to the large gap values, and offer novel functionalities in the design of the experiments determined by different dispersion for Andreev bound states as a function of the phase difference.

DOI: [10.1103/PhysRevB.86.144513](https://doi.org/10.1103/PhysRevB.86.144513)

PACS number(s): 73.23.-b, 73.20.-r, 74.20.Rp, 74.45.+c

### I. INTRODUCTION

Recently there has been an increasing interest in topological quantum computation based on Majorana bound states (MBSs).<sup>1,2</sup> Majorana fermions have been predicted in a wide class of low-dimensional solid-state devices. Many of these proposals make use of quasi-one-dimensional (quasi-1D) superconductors in contact with topological insulators<sup>3</sup> or quasi-one-dimensional materials with strong spin-orbit interactions.<sup>4-7</sup> Helical magnets<sup>8</sup> and other materials<sup>9-13</sup> are also considered. In this paper, we propose a quite distinctive heterostructure to observe topologically protected MBSs in a solid-state device. Our work rests on the physics of S/R/S hybrid structures in which R is a quasi-one-dimensional semiconductor nanowire (NW) with strong Rashba spin-orbit coupling (e.g., InAs or InSb) electrically connected to two conventional low- $T_c$  superconductor leads (S).<sup>4,5</sup> Superconductivity is induced in the spin-orbit coupled semiconductor by the proximity effect due to the superconducting electrodes. The coexistence of superconductivity and spin-orbit coupling is a key ingredient for the existence of MBSs at the interfaces between the R region and the superconducting S regions.

However, despite the considerable theoretical and experimental<sup>14</sup> efforts, some challenges still remain before a real device allowing isolation and manipulation of MBSs in such geometry can be realized. In particular, the difficulties of tuning the chemical potential of the semiconductor region  $\mu$ , controlling the disorder on the bulk gap, as well as optimizing the coupling between the different materials<sup>15-17</sup> make the realization of such devices extremely difficult.

All schemes proposed to date to generate MBSs substantially use conventional  $s$ -wave superconductors to induce superconductivity and a gap  $\Delta$  in the R nanowire.<sup>1</sup> The role of superconducting pairing is to relax number conservation, thus allowing for the mixing of particle and hole degrees of freedom. Zeeman spin splitting is required to halve the number of degrees of freedom at low energies, thus generating the elusive neutral (Majorana) excitation. A simple criterion to induce MBSs at S/R interfaces is given in terms of the applied magnetic field  $B_x$  oriented along the wire,  $\mu$  and  $\Delta$ . The inequality to be satisfied can be stated as  $B_x^2 > \mu^2 + \Delta^2$ .<sup>4</sup> Low

critical magnetic fields ( $H_c$ ) and low gap values characteristic of conventional low- $T_c$  superconductors substantially define the limits of the nominal range of dynamical parameters required to observe MBSs. Not only do  $H_c$  and  $\Delta$  enter into the criteria to stabilize MBSs, but they also endanger the feasibility of the experiment in case high magnetic fields are required. High-critical-temperature superconductors (HTS) may favor a completely different approach to experiments on MBSs, since HTS plaquettes/contacts (of even a few micron square) sustain superconductivity up to a few tenths of Tesla and induce robust superconductivity in a wide range of barrier materials. When conventional low- $T_c$  superconductors (LTS) (e.g., Nb) are considered, the large difference in the  $g$  factors for Nb ( $g_{\text{Nb}} \sim 1$ ) and InAs ( $g_{\text{InAs}} \sim 35$ ) implies that the in-plane magnetic field  $B \sim 0.1T$  can open a sizable Zeeman gap in InAs ( $V_x \leq 1K$ ). However, these conditions holds even more firmly in YBa<sub>2</sub>Cu<sub>3</sub>O<sub>7-x</sub> (YBCO) contacts because the YBCO gap is very stable with respect to magnetic fields, despite a doubling of the  $g$  factor ( $g_{\text{YBCO}} \sim 2$ ).

The paper is structured as follows. In Sec. II, we introduce the model Hamiltonian. In Sec. III, we report numerical results for the low-energy spectrum of the Hamiltonian of Eq. (4), clearly showing the presence of MBSs. In Sec. IV, we discuss the experimental feasibility of our proposal: in particular, in Sec. IV A, we propose an experiment aimed at observing an anomalous behavior of the critical current  $I_c$  as a function of the temperature; in Sec. IV B, we propose to explore tricrystal geometry to use the order parameter anisotropy as a key ingredient to probe MBSs; in Sec. IV C, we support with experimental evidence the actual possibility to use the proximity effect between high-temperature cuprate superconductors and semiconductors. In Sec. V, we report our conclusions. In the Appendix, we report an explicit calculation supporting the expected  $I_c(T)$  anomaly described in Sec. IV B.

### II. MODEL HAMILTONIAN

The induced gap in the NW can be considered of the order of the bare gap of the superconductor, projected along the wire direction, provided that the radius of the wire is

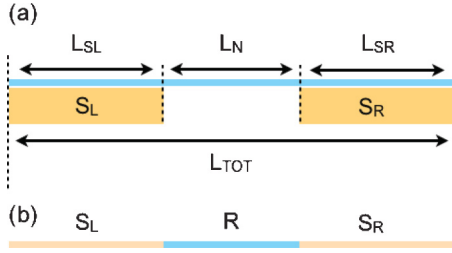


FIG. 1. (Color online) (a) Side view of the superconductor-InAs nanowire-superconductor heterostructure. (b) Scheme of the structure used for the effective one-dimensional model.

negligibly small with respect to the coherence length  $\xi$  of the superconducting material and that no sizable barriers are present at the interfaces. As recently pointed out in Ref. 15, the interface tunneling between different materials renormalizes the induced gap to  $\tilde{\Delta}_i = (1 - Z)\Delta_i$ , where  $Z \sim (1 + \pi\rho_0|V_{\text{hop}}|^2/\Delta_i)^{-1}$  is the quasiparticle weight,  $V_{\text{hop}}$  mimics the electron hopping between the superconductor and the NW, and  $\rho_0$  is the density of states of the superconductor at the Fermi energy. The better is the coupling with a larger  $V_{\text{hop}}$ , the smaller becomes  $Z$  and the larger is the induced gap.  $Z$  also renormalizes the whole NW Hamiltonian,  $H_{\text{NW}} \rightarrow \tilde{H}_{\text{NW}} = ZH_{\text{NW}}$ , which means that, by the same token, all the NW Hamiltonian parameters are effectively reduced when  $V_{\text{hop}}$  increases. When taking the renormalization into account in the model that we discuss below, the criterion for the appearance of the topologically nontrivial phase becomes

$$Z^2(B^2 - \mu^2) > (1 - Z)^2 \max(|\Delta_L|^2, |\Delta_R|^2). \quad (1)$$

This renormalization effect requires caution in the nanostructure design and, interestingly enough, it can be fruitfully

exploited in the case of HTS proximity. A convenient tradeoff can be found by accepting a rather poor intermaterial coupling  $V_{\text{hop}}$ , due to the very large bare superconducting gap along the lobe direction, which is almost one order of magnitude larger than in conventional LTS. The nanowire mostly rules the scaling of the proximity effect<sup>18–20</sup> once good interface conditions are guaranteed between the HTS material and the barrier material,<sup>21,22</sup> and in this case the InAs nanowire<sup>23</sup> (see below). The magnetic field can be very high with negligible effects both on the superconducting properties of the HTS electrode and on the interface transparency.

Here we focus on other functionalities of HTS hybrid devices, which are offered by an anisotropic  $d$ -wave order parameter symmetry.<sup>24</sup> In  $d$ -wave systems, lobes in the excitation gap of amplitude 20 meV coexist with nodes, while in conventional  $s$ -wave superconductors, the gap value is  $\sim 1$  or  $< 1$  meV and uniform in all directions. In HTS contacts, the crystal axes orientations with respect to the nanowire can be chosen in order to maximize the proximity-induced  $\Delta$ . Different crystal orientations can be currently achieved by bicrystal or biepitaxial techniques.<sup>22</sup>

For the sake of simplicity, we model the system as an effective one-dimensional device composed of the NW of length  $L_N$  and two superconducting regions [see Fig. 1(b)], whose effective gaps differ not only in phase but also in their modulus, depending on the relative crystal orientation (see Fig. 2).

In the superconducting regions of the nanowire, spin-orbit interaction and superconductivity coexist. We assume that  $L_N \ll \xi \ll L_{\text{TOT}}$  in order to have penetration of superconductivity in the whole nanowire.

A Bogoliubov-De Gennes mean-field Hamiltonian fully accounts for superconductivity induced in the normal material by the proximity effect:

$$\begin{aligned} \mathcal{H}_S &= (H_0 - \mu N) + \int_{-\infty}^{\infty} dx [\Delta(x)\psi_{\uparrow}^{\dagger}(x)\psi_{\downarrow}^{\dagger}(x) + \text{H.c.}], \\ H_0 - \mu N &= \int_{-\infty}^{\infty} dx \psi_{\alpha}^{\dagger}(x) \left[ \left( -\frac{\partial_x^2}{2m^*} - \mu \right) I_2 + i\eta\sigma_y\partial_x + B_x\sigma_x \right]_{\alpha\beta} \psi_{\beta}(x), \end{aligned} \quad (2)$$

where  $x$  is the coordinate along the wire and  $\alpha, \beta = \uparrow, \downarrow$  denote the two components of the electronic fermionic fields.  $m^*$  and  $\eta$  are the effective mass and the Rashba spin-orbit coupling strength, respectively.  $B_x = g\mu_B B/2$  is the effective Zeeman spin-splitting energy. It is assumed that the magnetic field, chosen in the direction of the wire, does not induce any undesired orbital effect. The  $d_{x^2-y^2}$  superconductivity pairing is modeled as<sup>24</sup>

$$\Delta(x) = \begin{cases} \Delta_L = \Delta_0 \cos[2(\vartheta - \alpha_L)] & \text{for } x < -L_N/2, \\ 0 & \text{for } -L_N/2 \leq x \leq L_N/2, \\ \Delta_R = \Delta_0 e^{-i\phi} \cos[2(\vartheta - \alpha_R)] & \text{for } x > L_N/2. \end{cases} \quad (3)$$

Angles  $\alpha_{R,L}, \vartheta$  are defined in Fig. 2.  $\phi$  is a U(1) phase difference across the junction. Let us choose  $\vartheta$  to be zero. Depending on the relative orientation of the order parameters in the  $L, R$  regions with respect to the nanowire, a wealth of possibilities exist. For an effectively one-dimensional wire, we can set  $\alpha_L = 0$  with no loss of generality. By rotating

$\alpha_R$  from 0 to  $\pi/2$ , we can continuously explore all of the configurations from lobe-lobe (+/+) to lobe-antinode (+/-). Nodal configurations are not interesting here, as we need large superconducting gaps. As we are searching for MBSs, we will choose only a few angle configurations to demonstrate the main concepts.

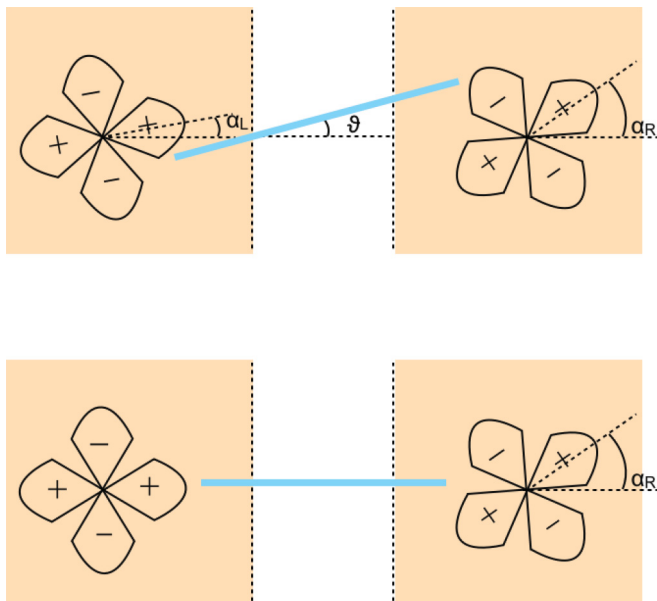


FIG. 2. (Color online) The top view sketch for different geometries. Configurations of the order parameter are determined by a suitable orientation of the electrodes and of the nanowire.

The Hamiltonian operator in  $\mathcal{H}_S$  can be recast in the compact form, in the basis  $\hat{\psi}(x) = [\psi_\uparrow(x), \psi_\downarrow(x), \psi_\downarrow^\dagger(x), -\psi_\uparrow^\dagger(x)]$ :

$$\tilde{H}_S/\eta = \left[ \left( -\frac{1}{2} \partial_x^2 - \mu \right) \sigma_0 + i \partial_x \sigma_y \right] \tau_z + B_x \sigma_x \tau_0 + \Delta(x) \tau_x. \quad (4)$$

It is a tensor product of matrices  $\tau_i \times \sigma_j$  with  $\{i, j\} \in \{0, 1, 2, 3\}$ , where  $\tau_i$  and  $\sigma_i$  are the usual Pauli matrices for  $i \neq 0$  and the  $I_2$  identity matrix for  $i = 0$ . They refer to the Nambu and spin degrees of freedom, respectively. A new space scale  $x \rightarrow \eta m^* x$  has been introduced, as well as energy scale  $\mu, B_x, \Delta \rightarrow \mu, B_x, \Delta / (m^* \eta^2)$ .

### III. MAJORANA BOUND STATES

The Hamiltonian of Eq. (4) has a topologically nontrivial phase whose boundary states are Majorana fermions, provided Eq. (1) is satisfied. The Hamiltonian parameters used here effectively include the quasiparticle renormalization weight  $Z$ . The topologically trivial phase is adiabatically deformable to the usual Andreev physics.<sup>25</sup> We calculate numerically the low-lying part of the energy spectrum by matching the eigenfunctions. In order to simplify the calculations, we take the limit  $L_N \sim 0$  by matching the wave function and its derivative at  $x = 0$ . As shown in Ref. 4, this assumption does not alter the generality of our results, as interaction terms among Majorana end states are neglected in our approach. The effects of a finite-size wire are shown for example in Ref. 26.

In Fig. 3, the dispersion relation of MBSs is shown as a function of the phase difference,  $\phi$ , between the superconducting pads. For  $\alpha_R < \pi/4$ , the Andreev levels show a single crossing at  $\phi = \pi$ . The odd number of crossings in the Andreev spectrum is the characteristic signature of the

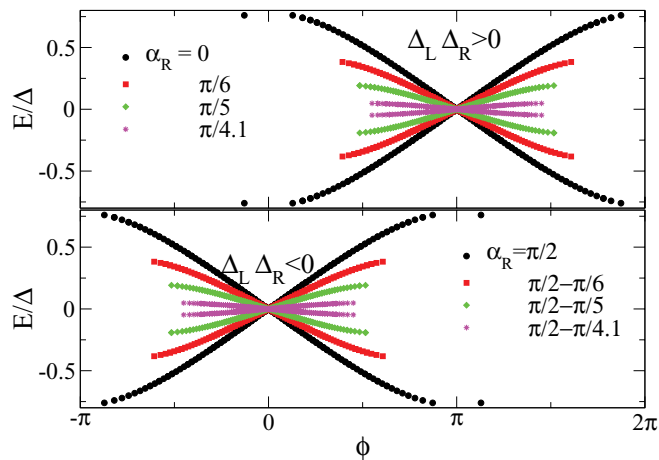


FIG. 3. (Color online) Energy spectrum of zero-energy Majorana bound states in the case of equal (opposite) sign gaps (in top and bottom panel, respectively).

topological nontrivial phase, consistent with that found with conventional  $s$ -wave superconductivity. However, the Andreev spectrum shows an unexpected behavior when  $\alpha_R > \pi/4$ , i.e., when the effective induced gaps have opposite signs. In this case, the crossing, which features the zero-energy MBS, is still present, but located at  $\phi = 0$ . This is specific to the  $d$ -wave order parameter. When  $\alpha_R < \pi/4$ , the gaps  $\Delta_L$  and  $\Delta_R$  have the same sign. Therefore, a phase difference of  $\pi$  between the two order parameters is required in order to have an inversion of the sign of the gap between the two regions,  $S_1$  and  $S_2$ . Provided that the appropriate condition for the parameters is met, the sign inversion, irrespective of the relative strength of the two gaps (and of the actual value of  $\alpha_R$ ), enforces the crossing to be localized at  $\phi = 0$ , and the Majorana excitation with it. Together with this change, the shape of the dispersion relation changes by changing  $\alpha_R$ , with an increase of the current  $I(\phi) = \partial E(\phi)/\partial \phi$  up to a maximum, when the gaps reach their maximum at  $\alpha_R = 0$  or  $\pi/2$ . The crossing only appears at  $\phi = 0, \pi$  because only at these points is the Hamiltonian real. Moreover, depending on the crystal relative arrangements, we can have a different dispersion for Andreev bound states as a function of the phase difference  $\phi$ . In both cases, a single crossing at zero energy appears, which reveals the presence of the MBS, at  $\phi = 0$  or  $\pi$  depending on the sign of the product  $\Delta_L \Delta_R$ .

### IV. EXPERIMENTAL FEASIBILITY

At present, the race to detect signatures of the elusive Majorana fermions in an  $S/NW/S$  structure is quite exciting.<sup>27–30</sup> A system exploiting  $d$ -wave electrodes, such as the one proposed in this work, can inspire hallmark experiments in the search for Majorana excitations. We briefly mention two different types of experiments, where it is natural to expect the merging of the physics of  $d$ -wave Josephson junctions, with their additional intrinsic possibility of manipulating the phase,<sup>24,31</sup> and of Majorana bound states. We conclude with a brief outlook on the progress in realizing and understanding HTS junctions, which make possible the realization of experiments aimed to detect Majorana fermions in HTS systems.

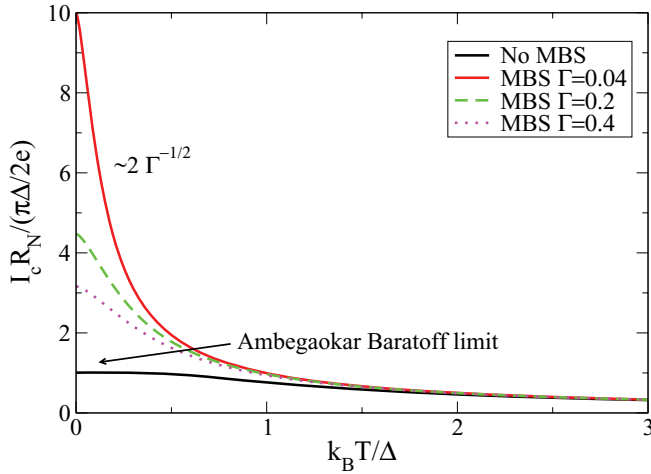


FIG. 4. (Color online)  $I_c R_N$  anomaly in the presence of MBSs for different values of the barrier transparency  $\Gamma$ . The trivial (Ambegaokar-Barotoff) limit is plotted as a comparison. The  $\Delta$  of the axes labels has to be intended as  $\Delta = \sqrt{\Delta_L \Delta_R}$ .

### A. Critical current anomaly

A  $d$ -wave-induced superconductivity offers a wider range of opportunities to discriminate the presence of the MBS. Andreev states induced by  $d$ -wave pairing are strongly sensitive to the geometry of the device. The characteristic increase of the  $I_c$  at the lower temperatures, used as a benchmark for the existence of the Andreev midgap state in HTS junctions,<sup>19</sup> is strongly suppressed when the width of the junction is reduced and the device enters in the quasi-1D limit. In the junctions devised in this work, an anomalous increase of  $I_c$  at low temperatures would persist in the 1D limit and would be even sharper the lower the barrier transparency is. In Fig. 4, we report the temperature dependence of  $I_c R_N$  for different values of the barrier transparency in the presence and the absence of a MBS. The numerical calculation used to obtain the results in Fig. 4 is shown in the Appendix. The  $I_c R_N$  product, in the presence of a MBS, diverges as  $1/\sqrt{\Gamma}$  at low temperatures,  $k_B T \ll \sqrt{\Delta_L, \Delta_R}$ , compared with the trivial case, which converges to the Ambegaokar Barotoff limit:

$$I_c R_N = \begin{cases} \frac{\pi \sqrt{\Delta_L \Delta_R}}{e \sqrt{\Gamma}} & \text{with MBS} \\ \frac{\pi \sqrt{\Delta_L \Delta_R}}{2e} & \text{no MBS.} \end{cases} \quad (5)$$

An experiment searching for  $I_c$  anomalies at low temperature would unambiguously signal a feature that can be correlated to the presence of Majorana fermions.<sup>32,33</sup>

### B. Experiments in tricrystal geometry

It is a distinctive property of ring structures with appropriate multicrystal arrangements to entail frustrated  $d$ -wave pairing ordering with trapped fractional fluxes in the ground state.<sup>24</sup> This has been one of the most exciting contributions of the Josephson effect on the debate on the nature of HTS, touching issues on time reversal symmetry breaking and the spontaneous nucleation of topological defects in phase transitions.<sup>21,24,34</sup> The possibility highlighted in this work, i.e., to have MBS localized at  $0-$  and  $\pi-$  junctions, depending on the phase configuration, has direct consequences on the

design of quantum coherent, topologically protected devices, which go beyond the simple experimental confirmation of this amazing new physics to enter the field of applications. We envisage the possibility of engineering quasidegenerate odd fermionic parity states, using a mesoscopic, charge-isolated island, formed by a  $d$ -wave tricrystal<sup>35</sup> topologically protected with respect to the excitations.

### C. Feasibility of hybrid HTS Josephson junctions

Performances of HTS Josephson junctions (JJs) in terms of yield and reproducibility are still limited when compared with those of LTS JJs.<sup>22</sup> However, significant progress has been recently registered both in the understanding of the phase dynamics in HTS JJs<sup>22,36–40</sup> and in the realization of HTS nanostructures<sup>41,42</sup> and of high-quality interfaces composed by oxides.<sup>21,43,44</sup> Escape dynamics has been used to demonstrate the occurrence of macroscopic quantum tunneling in GB biepitaxial<sup>36,37</sup> and intrinsic<sup>40</sup> JJs, and more recently to measure with accuracy the intrinsic dissipation of  $d$ -wave JJs also in the moderately damped regime.<sup>39</sup> These experiments demonstrate that local nodal quasiparticles (qps)<sup>24</sup> cannot spoil macroscopic quantum phenomena, and analogously suggest that nodal qps should be inefficient in producing a decay of the Majorana zero-energy excitation. Nodal qps are strictly at zero energy if traveling along given directions in a uniform system  $d$ -wave ordering. The presence of the Josephson barrier, inhomogeneity, or confined geometry should move those states to finite energy. In addition, by choosing an appropriate orientation of the  $d$ -wave lobes in the two superconducting regions, this phenomenon can be significantly controlled. Optical- and magnetoconductance measurements further support the notion of antinodal qps that is less disruptive for the quantum coherence at low temperatures than expected.<sup>45–47</sup>

More recent advances in patterning HTS nanostructures<sup>41,42</sup> opens alternative perspectives to adequately support the progress achieved in mastering high-quality interfaces.<sup>21,43</sup> As a matter of fact, key concepts and technologies have been acquired and hybrid structures encompassing nanowires<sup>23</sup> or topological insulators<sup>48</sup> and HTS are now possible. InAs/YBCO prototype structures have already been tested with encouraging results<sup>23</sup> with designs different from those used for LTS systems.<sup>49</sup>

### V. CONCLUDING REMARKS

It is well established that in order to obtain MBSs, in S/R/S heterostructures, the magnetic field should dominate over the superconductivity. Still, a sizable superconducting gap is needed, as the smaller energy between  $V_z$  and  $\Delta$  sets the minimum energy sufficient to wash out the topological protection of the Majorana excitation. In this respect, HTS appear to offer more chances in stabilizing MBSs.  $d$ -wave systems can offer novel functionalities in the design of the experiments determined by different dispersion for Andreev bound states as a function of the phase difference.

### ACKNOWLEDGMENTS

We acknowledge important discussions with D. Bercioux, P. Brouwer, M. Cuoco, P. Gentile, D. Urban, and F. von

Oppen. Financial support from FP7/2007-2013 under Grant No. 264098 - MAMA (Multifunctioned Advanced Materials and Nanoscale Phenomena), MIUR-Italy by Prin-project 2009 “Nanowire high critical temperature superconductor field-effect devices,” and European “SOLID” Project are gratefully acknowledged.

#### APPENDIX : CRITICAL CURRENT ANOMALY IN THE PRESENCE OF MAJORANA BOUND STATES

In  $d$ -wave Josephson junctions, at low temperatures, the critical current is strongly dependent on the possible presence of the midgap Andreev bound state (ABS) (for a review, see Refs. 19,20). The midgap state disappears when the device is strictly one dimensional. Otherwise, its energy dispersion as a function of the angle  $\theta$  of the wave vector  $k$  impinging at the interface and of phase difference  $\phi = \phi_L - \phi_R$  strongly depends on angle arrangements.

The  $d$ -wave gap order parameter for the left and right electrode can be written as

$$\Delta_i(\theta, \phi) = \Delta \cos(2\theta - 2\alpha_i) \exp(i\phi_i), \quad (\text{A1})$$

where  $\alpha_i$  ( $i = L, R$ ), which are the orientations of the left and right order parameter with respect to the direction orthogonal to the interface. In the Superconductor-Normal-Superconductor geometry, the Josephson current is determined by the ABSs of energy dispersion  $E(\theta, \phi)$ :

$$I \propto \pm \frac{e}{\hbar} \int_{-\pi/2}^{+\pi/2} \cos(\theta) d\theta \frac{dE(\theta, \phi)}{d\phi} \tanh[\beta E(\theta, \phi)]. \quad (\text{A2})$$

Two limiting cases can be highlighted (for simplicity, we will ignore intermediate cases here):

(1)  $[\alpha_L] = \alpha_R = 0$ . In this case, the ABSs are the same as in  $s$ -wave superconductivity.

(2)  $[\alpha_L] = \pm\alpha_R = \pi/4$ . In this case,  $|\Delta_L(\theta)| = |\Delta_R(\theta)| = |\Delta(\theta)| = \Delta \cos(2\theta - 2\alpha_L)$  and the energy dispersion of the

ABSs is

$$E(\theta, \phi) = \pm |\Delta(\theta)| \sqrt{\Gamma(\theta)} \sin(\phi/2), \quad (\text{A3})$$

where  $\Gamma$  is the barrier transparency. Here, the two dimensionality is crucial because the ballistic motion of antinodal carriers from the  $+$  to the  $-$  lobe (see Fig. 2) is required for the presence of the midgap state. Usually, a simple  $\theta$  dependence is assumed for  $\Gamma$  in the integral of Eq. (A2), which averages over the  $k$  components parallel to the interface.

The crucial difference between the case considered to date and that of a *topologically nontrivial one-dimensional wire*, in the hybrid structure, is the presence of the Majorana bound state (MBS) at zero energy. In this case, no matter how peaked the  $\Gamma(\theta)$  is along the wire direction  $\theta = 0$ , a contribution to the Josephson current comes from the energy dispersion of the Andreev bound states of the kind

$$E(\theta, \phi) = \sqrt{|\Delta_R \Delta_L|} \sqrt{\Gamma} \sin \left[ \frac{\phi}{2} - \frac{\pi}{2} \Theta(\Delta_R \Delta_L) \right], \quad (\text{A4})$$

which fits, with a good accuracy, the numeric results presented in Fig. 3. Therefore, even in one dimension, the presence of MBSs can give rise to localized zero-energy ABSs, reflected in an anomalous contribution to the subgap current. Real devices are expected to have a relatively low transmission coefficient. This is not a drawback for a setup involving HTS superconductors, as explained in the main text. However, low transparency is mostly favorable in order to distinguish whether a MBS is present or not. In fact, in the limit of low transparency, the  $I_c R_N$  product in the presence of a MBS diverges as  $1/\sqrt{\Gamma}$  at low temperatures. In the low-temperature limit  $k_B T \ll \sqrt{\Delta_L, \Delta_R}$ , we can derive the following analytical result:

$$I_c R_N = \begin{cases} \frac{\pi \sqrt{\Delta_L \Delta_R}}{e \sqrt{\Gamma}} & \text{with MBS} \\ \frac{\pi \sqrt{\Delta_L \Delta_R}}{2e} & \text{no MBS.} \end{cases} \quad (\text{A5})$$

<sup>1</sup>J. Alicea, *Rep. Prog. Phys.* **75**, 076501 (2012).

<sup>2</sup>A. Y. Kitaev, *Physics-Uspekhi* **44**, 131 (2001).

<sup>3</sup>J. C. Y. Teo and C. L. Kane, *Phys. Rev. B* **82**, 115120 (2010).

<sup>4</sup>R. M. Lutchyn, J. D. Sau, and S. Das Sarma, *Phys. Rev. Lett.* **105**, 077001 (2010).

<sup>5</sup>Y. Oreg, G. Refael, and F. von Oppen, *Phys. Rev. Lett.* **105**, 177002 (2010).

<sup>6</sup>M. Duckheim and P. W. Brouwer, *Phys. Rev. B* **83**, 054513 (2011).

<sup>7</sup>H. Weng, G. Xu, H. Zhang, S.-C. Zhang, X. Dai, and Z. Fang, *Phys. Rev. B* **84**, 060408 (2011).

<sup>8</sup>M. Kjergaard, K. Wölms, and K. Flensberg, [arXiv:1111.2129v1](https://arxiv.org/abs/1111.2129v1).

<sup>9</sup>J. Alicea, *Phys. Rev. B* **81**, 125318 (2010).

<sup>10</sup>L. Fu and C. L. Kane, *Phys. Rev. Lett.* **102**, 216403 (2009).

<sup>11</sup>A. R. Akhmerov, J. Nilsson, and C. W. J. Beenakker, *Phys. Rev. Lett.* **102**, 216404 (2009).

<sup>12</sup>Y. Tanaka, T. Yokoyama, and N. Nagaosa, *Phys. Rev. Lett.* **103**, 107002 (2009).

<sup>13</sup>J. Linder, Y. Tanaka, T. Yokoyama, A. Sudbø, and N. Nagaosa, *Phys. Rev. Lett.* **104**, 067001 (2010).

<sup>14</sup>E. S. Reich, *Nature* **483**, 7388 (2012).

<sup>15</sup>A. C. Potter and P. A. Lee, *Phys. Rev. B* **83**, 184520 (2011).

<sup>16</sup>R. M. Lutchyn, T. D. Stanescu, and S. Das Sarma, *Phys. Rev. Lett.* **106**, 127001 (2011).

<sup>17</sup>P. W. Brouwer, M. Duckheim, A. Romito, and F. von Oppen, *Phys. Rev. Lett.* **107**, 196804 (2011).

<sup>18</sup>J. Clarke, *Proc. R. Soc. A* **308**, 447 (1969); A. Kastalsky, A. W. Kleinsasser, L. H. Greene, R. Bhat, F. P. Milliken, and J. P. Harbison, *Phys. Rev. Lett.* **67**, 3026 (1991); A. A. Golubov and M. Yu. Kupryanov, *Sov. Phys. JETP* **69**, 805 (1989); S. Gueron, H. Pothier, N. O. Birge, D. Esteve, and M. H. Devoret, *Phys. Rev. Lett.* **77**, 3025 (1996); F. S. Bergeret and J. C. Cuevas, *J. Low Temp. Phys.* **153**, 304 (2008).

<sup>19</sup>Y. Tanaka and S. Kashiwaya, *Phys. Rev. Lett.* **74**, 3451 (1995); S. Kashiwaya and Y. Tanaka, *Rep. Prog. Phys.* **63**, 1641 (2000).

<sup>20</sup>T. Löfwander, V. S. Shumeiko, and G. Wendin, *Supercond. Sci. Technol.* **14**, R53 (2001).

- <sup>21</sup>H. Hilgenkamp, Ariando, H. J. H. Smilde, D. H. A. Blank, G. Rijnders, H. Rogalla, J. R. Kirtley, and C. C. Tsuei, *Nature (London)* **422**, 50 (2003); J. R. Kirtley, C. C. Tsuei, A. Ariando, C. J. M. Verwijs, S. Harkema, and H. Hilgenkamp, *Nature Phys.* **2**, 190 (2006).
- <sup>22</sup>F. Tafuri and J. R. Kirtley, *Rep. Prog. Phys.* **68**, 2573 (2005).
- <sup>23</sup>D. Montemurro, S. Roddaro, D. Massarotti, L. Sorba, F. Beltram, and F. Tafuri, MIUR Prin-project “Nanowire high critical temperature superconductor field-effect devices” (2011–2013) (unpublished).
- <sup>24</sup>C. C. Tsuei and J. R. Kirtley, *Rev. Mod. Phys.* **72**, 969 (2000).
- <sup>25</sup>G. E. Blonder, M. Tinkham, and T. M. Klapwijk, *Phys. Rev. B* **25**, 4515 (1982).
- <sup>26</sup>D. Pikulin and Y. Nazarov, *JETP Lett.* **9**, 639 (2011).
- <sup>27</sup>J. R. Williams, A. J. Bestwick, P. Gallagher, S. S. Hong, Y. Cui, A. S. Bleich, J. G. Analytis, I. R. Fisher, and D. Goldhaber Gordon, *Phys. Rev. Lett.* **109**, 056803 (2012).
- <sup>28</sup>V. Mourik, K. Zuo, S. Frolov, S. Plissard, E. Bakkers, and L. Kouwenhoven, *Science* **336**, 1003 (2012).
- <sup>29</sup>L. P. Rokhinson, X. Liu, and J. K. Furdyna, *Nature Phys.*, doi: 10.1038/nphys2429 (2012).
- <sup>30</sup>A. Das, Y. Ronen, Y. Most, Y. Oreg, M. Heiblum, and H. Shtrikman, *arXiv:1205.7073*.
- <sup>31</sup>H. Hilgenkamp, *Supercond. Sci. Technol.* **21**, 034011 (2008).
- <sup>32</sup>A. Zazunov and R. Egger, *Phys. Rev. B* **85**, 104514 (2012).
- <sup>33</sup>P. A. Ioselevich and M. V. Feigelman, *Phys. Rev. Lett.* **106**, 077003 (2011).
- <sup>34</sup>J. R. Kirtley, C. C. Tsuei, and F. Tafuri, *Phys. Rev. Lett.* **90**, 257001 (2003).
- <sup>35</sup>P. Lucignano, A. Mezzacapo, F. Tafuri, and A. Tagliacozzo (unpublished).
- <sup>36</sup>T. Bauch, F. Lombardi, F. Tafuri, A. Barone, G. Rotoli, P. Delsing and T. Cleason, *Phys. Rev. Lett.* **94**, 087003 (2005).
- <sup>37</sup>G. Rotoli, T. Bauch, T. Lindstrom, D. Stornaiuolo, F. Tafuri, and F. Lombardi, *Phys. Rev. B* **75**, 144501 (2007).
- <sup>38</sup>D. Stornaiuolo, G. Papari, N. Cennamo, F. Carillo, L. Longobardi, D. Massarotti, A. Barone, and F. Tafuri, *Supercond. Sci. Technol.* **24**, 045008 (2011).
- <sup>39</sup>L. Longobardi, D. Massarotti, D. Stornaiuolo, L. Galletti, G. Rotoli, F. Lombardi, and F. Tafuri, *Phys. Rev. Lett.* **109**, 050601 (2012).
- <sup>40</sup>K. Inomata, S. Sato, K. Nakajima, A. Tanaka, Y. Takano, H. B. Wang, M. Nagao, H. Hatano, and S. Kawabata, *Phys. Rev. Lett.* **95**, 107005 (2005); X. Y. Jin, J. Lisenfeld, Y. Koval, A. Lukashenko, A. V. Ustinov, and P. Muller, *ibid.* **96**, 177003 (2006).
- <sup>41</sup>D. Stornaiuolo, G. Rotoli, K. Cedergren, D. Born, T. Bauch, F. Lombardi, and F. Tafuri, *J. Appl. Phys.* **107**, 11390 (2010); D. Gustafsson, H. Pettersson, B. Iandolo, E. Olsson, T. Bauch, and F. Lombardi, *Nano Lett.* **10**, 4824 (2010); J. Nagel, K. B. Konvalenko, M. Kemmler, M. Turad, R. Werner, E. Kleisz, S. Menzel, R. Klingeler, B. Buchner, R. Kleiner, and D. Koelle, *Supercond. Sci. Technol.* **24**, 015015 (2011).
- <sup>42</sup>Ke Xu and J. R. Heath, *Nano Lett.* **8**, 3845 (2008); P. Mohanty, J. Y. T. Wei, V. Ananth, P. Morales, and W. Skocpol, *Physica C* **666**, 408 (2004); G. Papari, F. Carillo, D. Stornaiuolo, L. Longobardi, F. Beltram, and F. Tafuri, *Supercond. Sci. Technol.* **25**, 035011 (2012); F. Carillo, G. Papari, D. Stornaiuolo, D. Born, D. Montemurro, P. Pingue, F. Beltram, and F. Tafuri, *Phys. Rev. B* **81**, 054505 (2010); I. Sochnikov, A. Shaulov, Y. Yeshurun, G. Logvenov, and I. Bozovic, *Nature Nanotechnol.* **5**, 516 (2010); I. Sochnikov, I. Bozovic, A. Shaulov, and Y. Yeshurun, *Phys. Rev. B* **84**, 094530 (2011). F. Fittipaldi, A. Vecchione, R. Ciancio, S. Pace, M. Cuoco, D. Stornaiuolo, D. Born, F. Tafuri, E. Olsson, S. Kittaka, H. Yaguchi, and Y. Maeno, *Europhys. Lett.* **83**, 27007 (2008).
- <sup>43</sup>I. Bozovic, G. Logvenov, M. A. J. Verhoeven, P. Caputo, E. Goldobin, and T. H. Geballe, *Nature (London)* **422**, 873 (2003); I. Bozovic, G. Logvenov, M. A. J. Verhoeven, P. Caputo, E. Goldobin, and M. R. Beasley, *Phys. Rev. Lett.* **93**, 157002 (2004).
- <sup>44</sup>A. Ohtomo and H. Y. Hwang, *Nature (London)* **427**, 423 (2004); M. Salluzzo, G. Ghiringhelli, J. C. Cezar, N. B. Brookes, G. M. De Luca, F. Fracassi, and R. Vaglio, *Phys. Rev. Lett.* **100**, 056810 (2008); J. Mannhart and D. G. Schlom, *Science* **327**, 1607 (2010).
- <sup>45</sup>A. Tagliacozzo, F. Tafuri, E. Gambale, B. Jouault, D. Born, P. Lucignano, D. Stornaiuolo, F. Lombardi, A. Barone, and B. L. Altshuler, *Phys. Rev. B* **79**, 024501 (2009).
- <sup>46</sup>P. Lucignano, D. Stornaiuolo, F. Tafuri, B. L. Altshuler, and A. Tagliacozzo, *Phys. Rev. Lett.* **105**, 147001 (2010).
- <sup>47</sup>N. Gedik, J. Orenstein, R. Liang, D. A. Bonn, and W. N. Hardy, *Science* **300**, 1410 (2003).
- <sup>48</sup>P. Zareapour, A. Hayat, S. Y. F. Zhao, M. Kreshchuk, A. Jain, D. C. Kwok, N. Lee, S.-W. Cheong, Z. Xu, A. Yang, G. D. Gu, S. Jia, R. J. Cava, and K. S. Burch, *Nature Commun.*, doi: 10.1038/ncomms2042 (2012).
- <sup>49</sup>Y. J. Doh, J. A. van Dam, A. L. Roest, E. P. A. M. Bakkers, L. P. Kouwenhoven, and S. De Franceschi, *Science* **309**, 272 (2005); J. Xiang, A. Vidan, M. Tinkham, R. M. Westervelt, and C. M. Lieber, *Nature Nanotech.* **1**, 208 (2006).